

# Synergy between Angiostatin and Endostatin: Inhibition of Ovarian Cancer Growth<sup>1</sup>

Yumi Yokoyama, Mohanraj Dhanabal, Arjan W. Griffioen, Vikas P. Sukhatme, and S. Ramakrishnan<sup>2</sup>

Department of Pharmacology [Y. Y., S. R.], Obstetrics and Gynecology, and Comprehensive Cancer Center [S. R.], University of Minnesota, Minneapolis, Minnesota 55455; Renal Division, Beth Israel Deaconess Medical Center, Harvard Medical School, Boston, Massachusetts 02215 [M. D., V. P. S.]; and Tumor Angiogenesis Laboratory, Department of Internal Medicine, University Hospital Maastricht, Maastricht, The Netherlands [A. W. G.]

## ABSTRACT

Ovarian cancer is the leading cause of fatality among gynecological malignancies. Ovarian cancer growth is angiogenesis-dependent, and an increased production of angiogenic growth factors such as vascular endothelial growth factor is prognostically significant even during early stages of the disease. Therefore, we investigated whether antiangiogenic treatment can be used to inhibit the growth of ovarian cancer in an experimental model system. Mouse angiostatin (kringle 1–4) and endostatin were expressed in yeast. Purified angiostatin and endostatin were then used to treat established ovarian cancers in athymic mice. These studies showed that both angiostatin and endostatin inhibited tumor growth. However, angiostatin treatment was more effective in inhibiting ovarian cancer growth when compared with endostatin in parallel experiments. Residual tumors obtained from angiostatin- and endostatin-treated animals showed decreased number of blood vessels and, as a consequence, increased apoptosis of tumor cells. Subsequently, the efficacy of a combined treatment with angiostatin and endostatin was investigated. In the presence of both angiostatic proteins, endothelial cell proliferation was synergistically inhibited. Similarly, a combination regimen using equal amounts of angiostatin and endostatin showed more than additive effect in tumor growth inhibition when compared with treatment with individual angiostatic protein. These studies demonstrate synergism between two angiostatic molecules and that antiangiogenic therapy can be used to inhibit ovarian cancer growth.

## INTRODUCTION

Tumor growth and metastasis require neovascularization, the process by which new blood vessels are formed from preexisting host vasculature (1). Neovascularization is a complex process involving proteolysis of basement membrane, endothelial cell migration, proliferation, and matrix remodeling. Recent studies have shown that several growth factors such as FGFs<sup>3</sup> (acidic FGF, bFGF) (2), VEGF (3), and angiopoietins (4) participate either alone or in combination to coordinate the formation of new blood vessels. Apart from pathological conditions (malignancy, retinopathy), angiogenesis regularly occurs in female reproductive tissues such as ovaries and endometrium. Positive and negative mediators of angiogenesis, probably regulated by hormonal changes, orchestrate the cyclical induction and regression of new blood vessels in ovaries (corpus luteum). At least in

ovaries, angiopoietin 2 seems to play a crucial role in the regression of blood vessels (5).

Etiology of ovarian cancer is not completely understood. Epidemiological studies suggest that ovarian cancer risk is associated with ovulatory cycle (6) and artificial induction of ovulation in infertile patient (7). A vast majority of ovarian cancers arise from the single layer of epithelium surrounding the ovaries (8, 9). Ovarian cancer growth is angiogenesis-dependent (10, 11), and secretion of proangiogenic growth factors such as VEGF is of prognostic value (12, 13). In addition to inducing tumor angiogenesis, VEGF is also a contributing factor in the formation of malignant ascites in ovarian cancer (14, 15). Accumulation of ascites is a characteristic of ovarian cancer. Ascites fluid provides an ideal microenvironment for tumor growth and micrometastasis of the peritoneal wall. After surgical debulking of the primary tumor and ascites drainage, increased growth of metastatic nodules has been observed in ovarian cancer patients (16–18). In fact, O'Reilly *et al.* (19, 20) discovered angiostatin based on a similar phenomenon in mice bearing a transplantable tumor.

Angiostatin is a proteolytic fragment of plasminogen comprising the first 4-kringle domains. It was first identified as a natural inhibitor of angiogenesis in the serum and urine of tumor-bearing mice (21). Since then, angiostatin has been used to inhibit growth of many experimental tumors in animals using either human (22–25) or mouse tumor cell lines (26, 27). In parallel to the discovery of angiostatin, O'Reilly *et al.* (28) also identified endostatin, a proteolytic fragment of collagen type XVIII. Endostatin is a potent inhibitor of angiogenesis and was isolated from a mouse hemangioendothelioma cell line. Recombinant endostatin made in bacteria has been shown to inhibit growth of tumors (29, 30) and to lead to the regression of transplanted tumors (28). In addition to angiostatin and endostatin, a number of other endogenous proteins, including cytokines such as interleukin 4 (31), have been identified to have antiangiogenic activity. Retinal pigment-epithelium derived factor (32) and cleaved form of anti-thrombin (33) are recently described as potent inhibitors of angiogenesis and tumor growth. Thus far no one has investigated whether any of the angiostatic proteins can be used to treat gynecological malignancies. Using athymic mice transplanted with a human ovarian cancer cell line as an experimental model system, we investigated the relative potency of recombinant mouse angiostatin and endostatin. In this model system, angiostatin was more potent in inhibiting tumor growth than endostatin was. Furthermore, the combined treatment with both angiostatin and endostatin resulted in a synergistic antiangiogenic effect when compared with treatment with either angiostatin or endostatin alone.

## MATERIALS AND METHODS

**Cell Lines.** BCEs were obtained from Clonetics, Inc. (San Diego, CA). HUVE cells, passage 2, were kindly provided by Dr. Vercelotti (University of Minnesota, Minneapolis, MN). MA148, a human epithelial ovarian carcinoma cell line, was established at the University of Minnesota from a patient with stage III epithelial ovarian cystadenocarcinoma (34). The BCE and HUVE cells were maintained in endothelial cell growth medium (Clonetics) supplemented with 10 ng/ml human epidermal growth factor, 1  $\mu$ g/ml hydrocorti-

Received 9/29/99; accepted 2/18/00.

The costs of publication of this article were defrayed in part by the payment of page charges. This article must therefore be hereby marked *advertisement* in accordance with 18 U.S.C. Section 1734 solely to indicate this fact.

<sup>1</sup> Supported in part by grants from the United States Army Medical Research and Materiel Command, Shirley Ann Sparboe Endowment, Women's Health Fund, and Gynecological Oncology Group of America (to S. R.) and by a grant from the Dutch Cancer Society (to A. G.).

<sup>2</sup> To whom requests for reprints should be addressed, at 6-120 Jackson Hall, 321 Church Street, S.E., Department of Pharmacology, University of Minnesota, Minneapolis, MN 55455. Phone: (612) 624-1461; Fax: (612) 625-8408; E-mail: sunda001@maroon.tc.umn.edu.

<sup>3</sup> The abbreviations used are: FGF, fibroblast growth factor; bFGF, basic FGF; VEGF, vascular endothelial growth factor; BCE, bovine adrenal gland capillary endothelial cells; HUVE, human umbilical vein endothelial; PMSF, phenylmethylsulfonyl fluoride; MTT, 3-(4,5-dimethylthiazol-2-yl)-2,5-diphenyl-2,4-tetrazolium bromide; CAM, chick chorioallantoic membrane; CPAE, bovine pulmonary artery endothelial; FBS, fetal bovine serum.

sone, 12  $\mu\text{g/ml}$  bovine brain extract, 50  $\mu\text{g/ml}$  gentamicin sulfate, 50 ng/ml amphotericin-B, and 5% FBS. MA148 cells were cultured in RPMI 1640 (Life Technologies, Inc., Gaithersburg, MD) supplemented with 10% FBS, 100 units/ml penicillin, 100  $\mu\text{g/ml}$  streptomycin, and 2 mM L-glutamine.

**Purification of Recombinant Angiostatin and Endostatin.** Mouse angiostatin (kringle 1–4) and endostatin have been cloned and expressed in *Pichia pastoris* by Dhanabal *et al.* (30). *Pichia* clones were cultured in baffled shaker flasks and induced by methanol as previously described (35). For large-scale expression, fermentation was used. Culture supernatants from shaker flasks were precipitated with ammonium sulfate (50% saturation) and dialyzed against 10 mM Tris-HCl (pH 7.6), 0.5 mM PMSF. Cell-free fermentation product was first concentrated by ultrafiltration and then dialyzed against 10 mM Tris-HCl buffer (pH 7.6), 0.5 mM PMSF. Further purification was carried out by heparin affinity column. The heparin column was equilibrated with 10 mM Tris-HCl buffer (pH 7.6), 0.5 mM PMSF. Samples were applied to the column at a flow rate of 1.0 ml/min on a fast protein liquid chromatography (Amersham Pharmacia Biotech, Piscataway, NJ). After thorough washing to remove unbound proteins, the column was eluted with a continuous gradient of 0–1 M NaCl in 10 mM Tris-HCl (pH 7.6), 0.5 mM PMSF. Endostatin was eluted at about 0.5 M NaCl. Purified endostatin was analyzed on SDS-PAGE (12% acrylamide gel) under nonreducing conditions by mass spectrometry and N-terminal sequencing.

A mouse angiostatin expressing *Pichia* clone was cultured in baffled shaker flasks. Culture supernatants were precipitated with ammonium sulfate (50% saturation) and dialyzed against 50 mM phosphate buffer (pH 7.5), 0.5 mM PMSF. Samples were then applied onto a lysine ceramic column equilibrated with 50 mM phosphate buffer (pH 7.5), 0.5 mM PMSF. Matrix-bound proteins were then eluted from the column with a continuous gradient of 0–0.2 mM  $\epsilon$ -aminocaproic acid in 50 mM phosphate buffer. Purity of angiostatin was analyzed by SDS-PAGE (12%) under nonreducing conditions.

Purified materials were dialyzed against PBS [137 mM NaCl, 8.1 mM  $\text{Na}_2\text{HPO}_4$ , 2.68 mM KCl, 1.47 mM  $\text{KH}_2\text{PO}_4$  (pH 7.3)] and stored in aliquots at  $-70^\circ\text{C}$ .

**Endothelial Cell Proliferation Assay.** Essentially, the method described by O'Reilly *et al.* (28) was used. Confluent BCE and HUVE cells were trypsinized and resuspended in M199 (Life Technologies, Inc.) medium with 5% FBS. Cells were then seeded into gelatinized, 96-well culture plates at a density of 5000 cells/well. After 24 h, different concentrations of angiostatin and/or endostatin were added. Twenty minutes later, cultures were treated with 5 ng/ml of bFGF (Life Technologies, Inc.) in the presence of 1  $\mu\text{g/ml}$  heparin. The viability of the control and the treated cells was determined by the MTT (Sigma Chemical Co., St. Louis, MO) colorimetric assay (36) after 72 h of incubation. MTT assay actually determines the metabolic activity of mitochondria and correlates well with the number of viable cells (36). This assay has been previously used to evaluate endothelial cell proliferation (37).

**CAM Assay.** The ability of mouse endostatin and angiostatin to inhibit angiogenesis *in vivo* was first tested in a CAM assay. Three-day-old fertilized White Leghorn eggs were incubated at  $37^\circ\text{C}$  for 4 days with rotating everyday. A window (1  $\times$  2 cm) was gently cut on day 7. On day 9, sterilized silicon rings (1 cm diameter, 1 mm thickness) were placed on the CAM. Ten micrograms of endostatin or angiostatin were added inside the rings every day for 3 days. Control CAMs were treated similarly with sterile saline. At the end of the experiment, CAMs were fixed with 10% neutral buffered formalin and photographed using a digital camera.

**Tumor Growth Inhibition Studies.** Female athymic nude mice (6–8 weeks old) were purchased from the National Cancer Institute and allowed to acclimatize to local conditions for 1 week. Logarithmically growing human ovarian carcinoma cells were harvested by trypsinization and were suspended in fresh medium at a density of  $2 \times 10^7$  cells/ml. One hundred microliters of the single-cell suspension was then injected s.c. into the flanks of mice. When the tumors became visible (7 days after inoculation), mice were randomized into four groups. One group was injected with mouse endostatin s.c. at a dose of 20 mg/kg/day for 30 days. A second group of mice was treated with angiostatin at the same dose. A third group of mice was treated with a combination of mouse endostatin (20 mg/kg/day) and angiostatin (20 mg/kg/day) to evaluate the effect of combination therapy. A control group of mice (fourth) was treated with sterile PBS under similar conditions. All injections were given s.c. at the neck, which is about 3 cm away from the growing tumor mass. Tumor growth was monitored by periodic caliper measurements. Tumor

volume was calculated by the following formula: tumor volume ( $\text{mm}^3$ ) =  $(a \times b^2)/2$ , where a = length in mm and b = width in mm.

Statistical significance between control and treated groups was determined by Student's *t* test. A minimum of five animals was used in each group and the experiments were repeated at least twice. Data from independent experiments were pooled for statistical analysis.

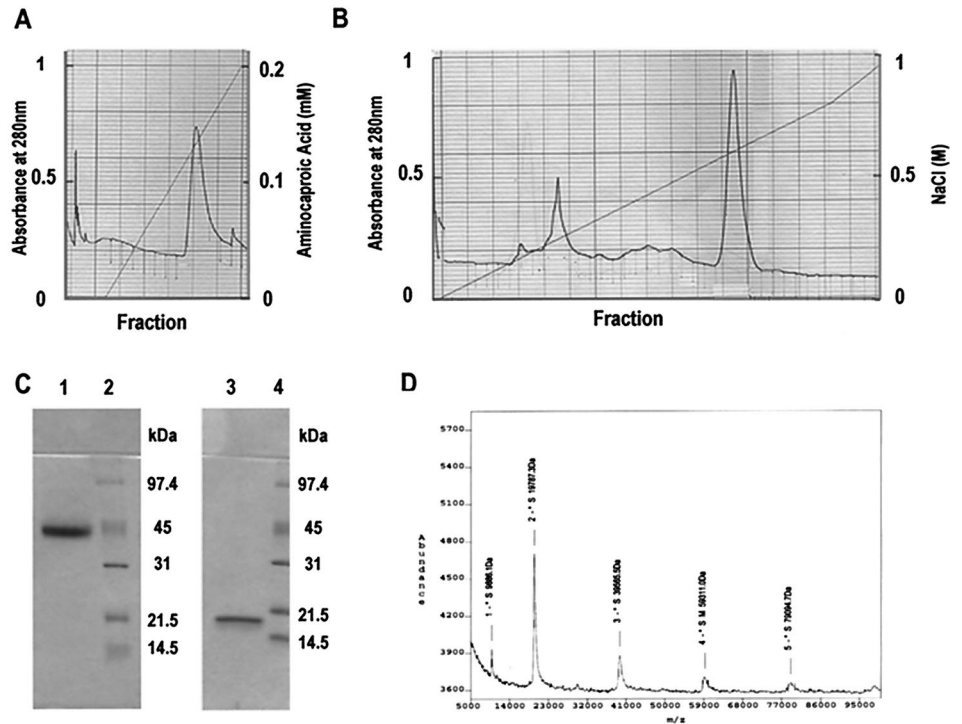
**Determination of Vessel Density and Apoptosis.** To determine the effect of antiangiogenic treatments on vessel density and apoptosis, residual tumors were surgically resected and snap frozen. Cryostat sections (4  $\mu\text{m}$ ) of tumors were then treated with PBS containing 0.1% BSA and 5% human serum to block nonspecific binding (background). Sections were then incubated with 1:50 dilution of an anti-CD31 (mouse) monoclonal antibody conjugated to phycoerythrin (Sigma). After 1 h incubation at room temperature, sections were washed thoroughly with PBS containing 0.1% BSA and 5% human serum and were then examined under an Olympus (New Hyde Park, NY) BX-60 fluorescence microscope at  $\times 10$  magnification. Images were captured by the Metamorph program for analysis. Detection of apoptosis was carried out by using an *In Situ* Cell Death Detection Kit (Boehringer Mannheim, Indianapolis, IN) following the manufacturer's protocol. Parts of the tumor samples were also fixed in 10% neutral buffered formalin and processed for histochemistry (H&E staining).

## RESULTS

**Expression and Purification of Recombinant Mouse Angiostatin and Endostatin.** The *Pichia* expression system was used to prepare recombinant mouse angiostatin and endostatin in soluble form (30). Purification of angiostatin and endostatin was carried out by affinity chromatography using lysine and heparin linked to ceramic particles (matrix) respectively. A typical purification run is shown in Fig. 1, A and B. Mouse angiostatin was eluted as a single homogenous peak and contained pure protein with <5% contamination in SDS-PAGE (Fig. 1C). The apparent molecular weight of the purified angiostatin was about  $M_r$  42,000 as per the relative mobility on SDS-PAGE under nonreducing condition. Angiostatin (residues Val<sub>98</sub>-Gly<sub>458</sub> of plasminogen) encompassing kringle 1–4 (19, 24) has a total of 361 amino acid residues. Peptide composition analysis (MacVector, 4.1.5) predicts a theoretical molecular weight of  $M_r$  41,100, which is very close to the observed value. Endostatin was eluted from the affinity matrix at 500 mM NaCl as a single peak containing a  $M_r$  20,000 protein. The preparation of endostatin showed small but detectable levels of dimers in SDS-PAGE by silver staining and Western blotting (data not shown). Typically, angiostatin was expressed in higher quantity than endostatin in shaker flasks. Yields for angiostatin varied between 15 and 20 mg/L. In contrast, endostatin was expressed at a lower level (5–8 mg/L). A batch fermentation run provided about 50–60 mg/L of mouse endostatin from a working volume of 6 L. Purified endostatin was analyzed by mass spectrometry. Endostatin showed a molecular weight of  $M_r$  19,787. In addition, two smaller peaks corresponding to a molecular weight of  $M_r$  39,500 and  $M_r$  59,300 were also observed (Fig. 1D). The higher molecular weight peaks correspond to dimeric and trimeric forms of endostatin. Every batch of endostatin showed a similar profile. However, the proportion of individual component cannot be accurately determined from mass spectrometry (inherent limitation). On the basis of SDS-PAGE, the relative amount of higher molecular weight endostatin was <5%. Each batch of endostatin was analyzed for biological activity. For *in vivo* studies, a single batch was used for each experiment.

**Biological Activity of Recombinant Angiostatin and Endostatin.** Antiproliferative activity *in vitro* and antiangiogenic activity *in vivo* were used to evaluate the biological activity of the recombinant proteins. Inhibition of endothelial cell proliferation was determined using BCE and HUVE cells. Purified angiostatin and endostatin inhibited HUVE cell proliferation by 50% ( $\text{IC}_{50}$ ) at concentrations of 10  $\mu\text{g/ml}$  and 8.6  $\mu\text{g/ml}$ , respectively. Interestingly, when cultures

Fig. 1. Purification of mouse angiostatin and endostatin expressed in yeast, and SDS-PAGE analysis. *A*, Mouse angiostatin was purified using an affinity column, lysine linked to ceramic beads. Angiostatin was eluted by continuous gradient of  $\epsilon$ -aminocaproic acid (0–0.2 M). *B*, Mouse endostatin was purified using a heparin affinity chromatography and was eluted by continuous gradient of NaCl (0–1 M). *C*, Purified mouse angiostatin and endostatin were analyzed by electrophoresis in 12% polyacrylamide gel. *Lane 1*, Purified mouse angiostatin; *Lane 3*, purified mouse endostatin; *Lanes 2 and 4*, molecular weight markers. *D*, Mass spectrum of endostatin.



were simultaneously exposed to both endostatin and angiostatin, there was a pronounced inhibition of HUVE cells. A representative experiment is shown in Fig. 2A. Combination of angiostatin and endostatin inhibited proliferation by 50% at 0.57  $\mu\text{g}/\text{ml}$  ( $\text{IC}_{50}$ ). When compared with  $\text{IC}_{50}$  of individual treatment with angiostatin and endostatin (10 and 8.6  $\mu\text{g}/\text{ml}$ , respectively), the combined treatment showed >16-fold improvement in antiproliferative activity. We also tested the direct effect of angiostatin and endostatin on tumor cells such as MA148; SIHA, a human cervical cancer cell line; and HUFF, a human foreskin fibroblast cell line. Neither endostatin nor angiostatin inhibited the proliferation of these cell lines (data not shown). To determine whether the increased antiproliferative effect was synergistic or additive, isobolographic analysis was carried out. Different combinations of concentrations of angiostatin and endostatin were added to BCE

cultures either alone or together. From the dose-response curves,  $\text{IC}_{40}$  (a concentration at which BCE proliferation was inhibited to 40% of control) values were calculated. These values were then used to generate isobologram. Data in Fig. 2B show the effect of combination treatment. When compared with the theoretical line (diagonal) representing additive effect, all of the values from combination treatment are found to be distributed below (to the left of) the theoretical line. If angiostatin and endostatin acted additively, the values would have fallen directly on the diagonal line. On the other hand, a competitive effect between angiostatin and endostatin would have distributed the values above (to the right) the theoretical line. The results clearly demonstrate that combination of angiostatin and endostatin synergistically inhibits proliferation of endothelial cells.

**Inhibition of Angiogenesis.** To study *in vivo* antiangiogenic activity, endostatin and angiostatin were tested in a CAM assay. This assay system is based on developmental angiogenesis and is used to get an initial indication of angiostatic activity prior to testing *in vivo* tumor growth models. In a modified CAM assay, 9-day-old fertilized eggs were used. Angiostatin and endostatin were applied directly on the CAM within the confined space of silastic rings. In this assay system, both endostatin and angiostatin inhibited development of new embryonic blood vessels without affecting preexisting vasculature (Fig. 3).

**Inhibition of Ovarian Cancer Growth.** To test whether mouse angiostatin and mouse endostatin could inhibit ovarian cancer growth, we used the human ovarian carcinoma cell line MA148. This model system has been previously used in our laboratory to determine the effect of anti-VEGF antibodies on tumor angiogenesis and tumor growth (38). MA148 cells were grown s.c. so that changes in tumor growth could be easily monitored. Tumors were first allowed to establish for 7 days. At this time, small palpable tumor nodules could be easily seen under the skin. Mice were then randomized and divided into groups. Angiostatin and endostatin were administered s.c. for a period of 30 days. Two independent experiments were carried out. Data in Fig. 4 show the relative effect of angiostatin and endostatin therapy. Angiostatin was found

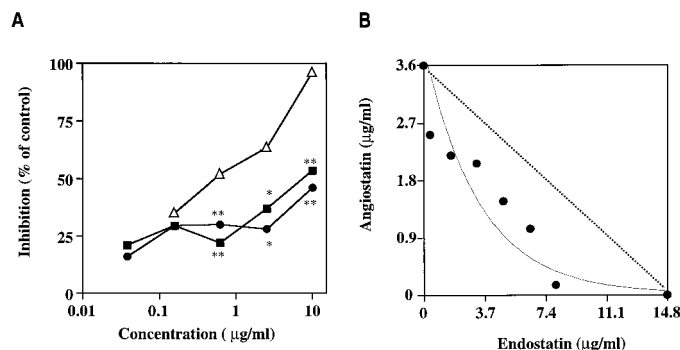


Fig. 2. Endothelial cell proliferation assay. Purified mouse angiostatin and endostatin were tested for their antiproliferative ability using HUVE cells (*A*). Medium including 5% of FBS with 5 ng/ml of bFGF was used. ■, endostatin; ●, angiostatin; and △, combined addition of angiostatin and endostatin. Viability of cells was determined by MTT assay. One hundred percent inhibition is equal to complete reduction of bFGF-induced endothelial cell proliferation to control cells cultured in the absence of bFGF. *B*, Combination effect of angiostatin and endostatin on BCE cells was plotted in an isobologram. The dotted line shows the theoretical line representing additive effect. Each value is derived from a dose-response curve and represents a dose required to elicit 40% inhibition ( $\text{IC}_{40}$ ) of BCE proliferation. Statistical significance between endostatin or angiostatin alone and their combination was determined using Student's *t* test. \*,  $P < 0.05$ ; \*\*,  $P < 0.01$ .

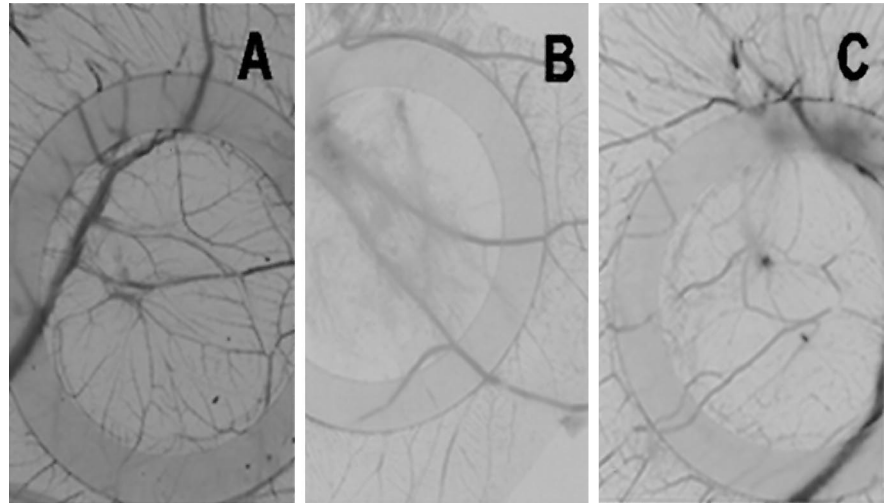


Fig. 3. Antiangiogenic effect of mouse angiostatin and endostatin on CAM assay. Ten micrograms of mouse angiostatin and endostatin in 50  $\mu$ l of sterile saline were applied onto the CAMs everyday for 3 days. Control CAMs received sterile saline. A, Control; B, angiostatin; C, endostatin.

to inhibit ovarian cancer growth better when compared with endostatin in parallel experiments. For example, after 2 weeks of treatment with angiostatin, a mean tumor volume of 200  $\text{mm}^3$  was observed. Under similar conditions, endostatin-treated animals showed a mean tumor volume of 362  $\text{mm}^3$ , whereas mean tumor volume of control mice was 589  $\text{mm}^3$ . Tumor growth was significantly reduced during the entire treatment period with angiostatin.

**Effect on Tumor Blood Vessels and Apoptosis.** To evaluate the consequence of antiangiogenic therapy, we examined the residual tumors histologically. Frozen tumor sections were immunohistochemically stained with an endothelial specific antibody against CD31. Immunofluorescence studies showed that angiostatin- or endostatin-treated tumors decreased the density of blood vessels (Fig. 5, A, D, and G). The same frozen sections were also analyzed for changes in the viability of tumor cells using a TUNEL assay (Fig. 5, B, E, H). Serial sections of each tumor were also stained by H&E to assess necrotic changes (Fig. 5, C, F, and I). When compared with control tumor sections, endostatin- and angiostatin-treated tumors showed pronounced increase in apoptosis. Increased incidence of apoptosis coincided with increase in calcification and necrosis of tumor tissue. However, histopathological analysis of normal tissues from the same animals did not show any increase in apoptosis or

necrosis (data not shown). Collectively, these results show that antiangiogenic therapy results in reduced tumor angiogenesis leading to apoptotic death of ovarian cancer cells.

**Synergistic Effect of Angiostatin and Endostatin on Ovarian Cancer Growth.** Because endothelial proliferation was inhibited better when angiostatin and endostatin were added together, we investigated in an independent study whether angiostatin treatment can be combined with endostatin to improve antitumor effect. Fig. 6 shows mean tumor volume on day 42. Endostatin and angiostatin alone showed inhibition of tumor growth by 5% and 57%, respectively, in this experiment. However, a combination of angiostatin and endostatin showed better antitumor activity with about 81% inhibition of tumor growth. Table 1 summarizes relative tumor volume of control and treated groups on three different time points. Combination therapy showed more than additive effect on tumor growth inhibition. On day 36, there was 1.34-fold improvement in antitumor activity in the combination group when compared with the expected additive effect. At this time point, endostatin alone inhibited tumor growth by 20% (fractional tumor volume, 0.797  $\text{mm}^3$ ) when compared with the control group. With time, there was a progressive improvement in antitumor activity. On day 42, angiostatin and endostatin combination group showed a 2-fold higher inhibition of tumor growth over additive effect (expected fractional tumor volume). In the present study, both angiostatic proteins were given together in a fixed schedule and dose. Therefore, the observed synergism can be further improved by modulating dosage and frequency of administration based on pharmacokinetics, distribution, and bioavailability.

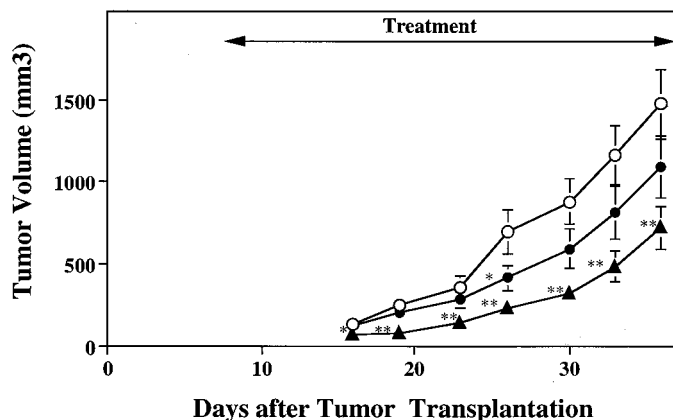


Fig. 4. Inhibition of ovarian cancer by angiostatin and endostatin. Human epithelial ovarian carcinoma cell line MA148 was injected s.c. into female, athymic mice. After 7 days, to allow tumor establishment, mice were treated with angiostatin and endostatin. Treatment was continued for 30 days.  $\circ$ , Control, PBS;  $\bullet$ , mouse endostatin;  $\blacktriangle$ , mouse angiostatin. Mean tumor volume was determined by caliper measurements. Data from two independent experiments were pooled and plotted. Statistical significance was determined using Student's *t* test. \*,  $P < 0.05$ ; \*\*,  $P < 0.01$ . The error bars indicate the SE.

## DISCUSSION

Recombinant forms of angiostatin and endostatin have been expressed in prokaryotic and eukaryotic cells (23, 28, 30). Bacterial expression systems have often resulted in insoluble proteins necessitating a refolding protocol. However, insoluble endostatin has been shown to be effective *in vivo*. Slow release of endostatin from the insoluble suspension coupled with proper refolding *in vivo* is suggested to be responsible for the potent inhibition of angiogenesis and tumor growth (28). Solubility problems can be avoided by expressing endostatin in other host cells such as yeast. Heterologous expression of mammalian proteins can sometimes result in altered post-translational modifications and heterogeneity at the termini. Indeed, amino terminal heterogeneity has also been observed in yeast-derived endostatin (39). In one instance, host (yeast) cells were genetically altered to reduce proteolytic heterogeneity in the carboxyl terminus of

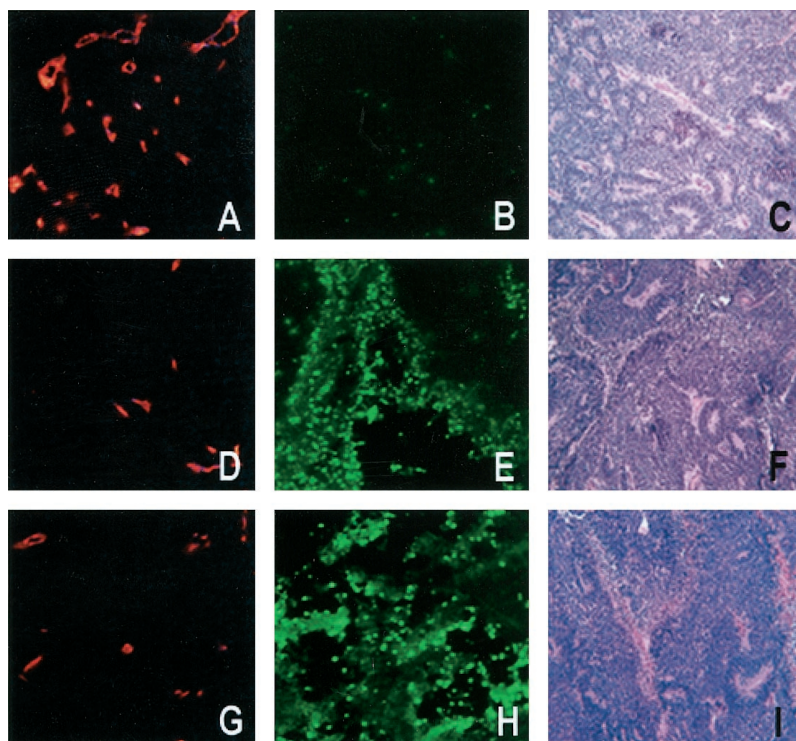


Fig. 5. Histochemical analysis. Residual tumors from angiostatin- and endostatin-treated groups were resected 4 days after the completion of treatment. A, D, and G, Vessel density as revealed by PE-labeled anti-CD31 antibody staining. B, E, and H, TUNEL assay. C, F, and I, H&E staining. A, B, and C, Control; D, E, and F, Angiostatin-treated tumor sections. G, H, and I, Endostatin-treated tumor sections.

endostatin (40). Sometimes processing of the termini can affect the biological activity of recombinant proteins. Proteolytic cleavage between histidine (H3) and glutamine (Q4) residues at the amino terminus has been observed in mouse endostatin. Such truncation results in the loss of the first three (HTH) residues at the amino terminus. These three residues are involved in tetrahedral complexing with a single atom of  $Zn^{2+}$  (39). Zinc binding and dimerization have been implicated in antitumor activity of endostatin. Endostatin preparation used in this study showed a homogeneous, major peak corresponding to a molecular weight of  $M_r$  19,787, which is slightly less than the expected size. Microsequencing of the amino terminus confirmed that the first three amino acid residues, HTH, were proteolytically cleaved in the mouse endostatin. The amino terminus started with a glutamine residue. Absence of the first two histidines (H1 and H3) is expected to affect zinc binding. The endostatin preparation used in the present study showed only a small fraction of dimeric and trimeric proteins by mass spectrometry. Despite the amino terminal processing, endostatin was very effective in inhibiting endothelial cell proliferation *in vitro* and angiogenesis *in vivo* (CAM). A recent study by Yamaguchi *et al.* (41) supports our finding that endostatin activity (*in vitro* and *in vivo*) may not be dependent on zinc binding. In this particular study, endostatin was genetically modified to eliminate the  $Zn^{2+}$  binding

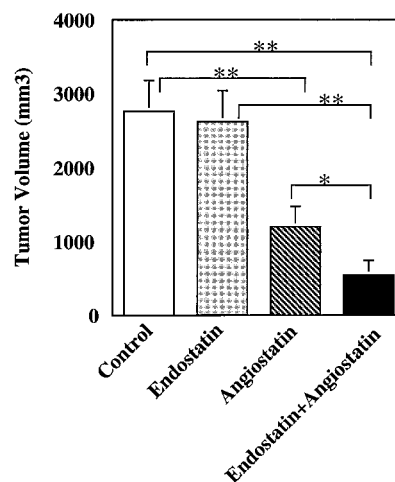


Fig. 6. Combination effect of mouse angiostatin and endostatin on ovarian tumor growth. Female, athymic mice transplanted with MA148 cells were treated by angiostatin and/or endostatin. Tumor sizes were measured 42 days after inoculation. Statistical significance was determined using Student's *t* test. \*,  $P < 0.05$ ; \*\*,  $P < 0.01$ . Error bars indicate SE.

Table 1 Combination therapy with angiostatin and endostatin

Day <sup>b</sup>	Fractional tumor volume (FTV) relative to untreated controls <sup>a</sup>		Combination treatment		Ratio of expected FTV/ observed FTV <sup>d</sup>
	Endostatin	Angiostatin	Expected <sup>c</sup>	Observed	
36	0.797	0.393	0.313	0.234	1.338
39	0.804	0.439	0.320	0.199	1.608
42	0.950	0.432	0.410	0.196	2.092

<sup>a</sup> FTV (mean tumor volume experimental)/(mean tumor volume control).

<sup>b</sup> Day after tumor cell transplantation.

<sup>c</sup> (Mean FTV of endostatin)  $\times$  (mean FTV of angiostatin).

<sup>d</sup> Obtained by dividing the expected FTV by the observed FTV. A ratio of  $>1$  indicates a synergistic effect, and a ratio of  $<1$  indicates a less than additive effect.

site. Such a construct was still biologically active. Structural features in angiostatin that are important for the antiangiogenic activity are not known. The basic kringle structure itself may be a requirement for angiostatic activity. For example, kringle 5 of plasminogen (42) as well as the kringle 2 of prothrombin (43) are potent inhibitors of endothelial cell proliferation. However, the definitive structure/function correlation has not been established yet. Further mutational studies can identify the regions of importance within the kringle region, which are important for angiostatic activity.

Potency of angiostatic molecules has been found to vary a lot depending on the cell type used. Ji *et al.* (42) reported that BCE cells are more sensitive than HUVE cells to kringle 5 in a migration assay. Dhanabal *et al.* (30) reported that CPAE cells are more sensitive than

other endothelial cell lines. Therefore, we compared the effect of angiostatin and endostatin on two different endothelial cells, BCE and HUVE cells. BCE cells were much more sensitive to both angiostatin and endostatin. We also tested CPAE and human microvascular endothelial cells. CPAE cells were as sensitive as BCE cells, and mouse microvascular endothelial cells were similar to HUVE cells (data not shown).

Angiostatin and endostatin effectively inhibited developmental angiogenesis *in vivo*. We used a modified CAM assay in which test solutions are applied directly onto a localized area of the CAM. In this method, the samples stay inside the rings, and new blood vessel formation inside the rings then can be compared with normal vasculature surrounding the ring. Another advantage of this method is that the blood vessels can be easily fixed by buffered formalin so that it is possible to cut CAMs out and observe them in detail. Direct application of angiostatin and endostatin expressed in yeast clearly inhibited actively growing blood vessels inside the ring. Vasculature outside the ring was not affected by this treatment.

Although angiostatin and endostatin have been tested in many tumor models, the relative potency has not been established in parallel experiments. Angiostatin is found to be effective against Lewis lung carcinoma at doses ranging from 1 mg/kg (24) and 50 mg/kg (44). Endostatin, on the other hand, is used in the same model in an insoluble form at a dose of 10 and 20 mg/kg (29). It is difficult to compare the relative potency because the rate of release of endostatin from the insoluble form is not determined. In the present study, we compared the relative antitumor effect of angiostatin and endostatin in soluble form against human ovarian carcinomas established in athymic mice. Both reagents were given at a similar dose and schedule. These studies showed that angiostatin was more potent in inhibiting ovarian cancer growth compared with endostatin. It is possible that the absence of zinc-binding residues could have contributed to the low antitumor activity of endostatin. However, endostatin was equally effective as angiostatin in inhibiting endothelial cell proliferation *in vitro* and developmental angiogenesis *in vivo*. Other reasons for the differences in antitumor activity could be due to tumor-dependent variations in the microenvironment affecting endothelial sensitivity. For example, it is possible that different types of tumors can secrete distinct sets of growth factors that can modulate the sensitivity of tumor vasculature to angiostatin and endostatin differently. Differences in pharmacokinetics and tissue distribution can also differentially alter bioavailability of angiostatin and endostatin. Angiostatin is expected to have a longer half-life than endostatin. Endostatin, with a molecular weight of  $M_r$  20,000, will be cleared from the circulation rapidly by renal filtration. Apart from the circulatory half-life, endostatin is observed to bind host vasculature, which can restrict its availability at tumor target site (45). Interaction with normal blood vessels can affect tissue distribution and will reduce bioavailability of endostatin. It will be possible to improve the efficacy of angiostatic molecules by (a) pharmacological approaches and (b) structural changes to increase half-life/bioavailability.

Angiostatin and endostatin are believed to act on endothelial cells by different mechanisms. Angiostatin has been recently shown to bind  $\alpha/\beta$  subunits of a membrane-bound ATP synthase (46). However, endostatin seems to affect levels of antiapoptotic proteins such as BCL-2 inside the cell (47). These studies suggest that upstream apoptotic signaling cascades of caspases are activated by endostatin treatment. Due to the nonoverlapping nature of the inhibitory pathways, treatment of endothelial cells with a combination of angiostatin and endostatin resulted in synergistic inhibition. Synergy between the two angiostatic molecules was confirmed by isobolographic analysis. Improved antiangiogenic activity was also reflected *in vivo* when tumor-bearing animals were treated with a combination of equal doses

of angiostatin and endostatin. Compared with expected additive effects, a 2-fold increase in antitumor activity was observed when mice were treated with equal doses of angiostatin and endostatin. The observed synergy between the two angiostatic proteins can be further improved by optimizing dosage and schedule of administration. These questions will be addressed in future studies using genetically redesigned second-generation angiostatic molecules. Whereas our current studies suggest a potential use of combination therapy using angiostatic proteins, one could also achieve better antitumor response by combining antiangiogenic therapy with other antitumor therapies (*e.g.*, chemo-radiation). For example, radiation therapy when combined with angiostatin showed potentiation of antitumor activity (25, 48). In another related strategy, antibodies to VEGF were used in combination with radiation therapy to achieve improved antitumor activity (49). Radiation induces elevated expression of VEGF as a survival factor from tumor cells. Therefore, neutralizing VEGF under these conditions resulted in better inhibition of tumor growth. In summary, our studies show for the first time that antiangiogenic therapy can be used to inhibit the growth of ovarian cancer and that angiostatin can synergize with endostatin in inhibiting tumor growth.

## REFERENCES

- Folkman, J. What is the evidence that tumors are angiogenesis dependent? *J. Natl. Cancer Inst.*, 82: 4–6, 1990.
- Kandel, J., Bossy-Wetzel, E., Radvanyi, F., Klagsbrun, M., Folkman, J., and Hanahan, D. Neovascularization is associated with a switch to the export of bFGF in the multistep development of fibrosarcoma. *Cell*, 66: 1095–1104, 1991.
- Ferrara, N., Houck, K., Jakeman, L., and Leung, D. W. Molecular and biological properties of the vascular endothelial growth factor family of proteins. *Endocr. Rev.*, 13: 18–32, 1992.
- Maisonpierre, P. C., Suri, C., Jones, P. F., Bartunkova, S., Wiegand, S. J., Radziejewski, C., Compton, D., McClain, J., Aldrich, T. H., Papadopoulos, N., Daly, T. J., Davis, S., Sato, T. N., and Yancopoulos, G. D. Angiopoietin-2, a natural antagonist for Tie2 that disrupts *in vivo* angiogenesis. *Science* (Washington DC), 277: 55–60, 1997.
- Goede, V., Schmidt, T., Kimmina, S., Kozian, D., and Augustin, H. G. Analysis of blood vessel maturation processes during cyclic ovarian angiogenesis. *Lab. Investig.*, 78: 1385–1394, 1998.
- Greene, M. H., Clark, J. W., and Blayney, D. W. The epidemiology of ovarian cancer. *Semin. Oncol.*, 11: 209–226, 1984.
- Rossing, M. A., Daling, J. R., Weiss, N. S., Moore, D. E., and Self, S. G. Ovarian tumors in a cohort of infertile women. *N. Engl. J. Med.*, 331: 771–776, 1994.
- Auersperg, N., Edelson, M. I., Mok, S. C., Johnson, S. W., and Hamilton, T. C. The biology of ovarian cancer. *Semin. Oncol.*, 25: 281–304, 1998.
- Berchuck, A., Elbendary, A., Havrilesky, L., Rodriguez, G. C., and Bast, R. C., Jr. Pathogenesis of ovarian cancers. *J. Soc. Gynecol. Investig.*, 1: 181–190, 1994.
- Olson, T. A., Mohanraj, D., Carson, L. F., and Ramakrishnan, S. Vascular permeability factor gene expression in normal and neoplastic human ovaries. *Cancer Res.*, 54: 276–280, 1994.
- Yoneda, J., Kuniyasu, H., Crispens, M. A., Price, J. E., Bucana, C. D., and Fidler, I. J. Expression of angiogenesis-related genes and progression of human ovarian carcinomas in nude mice. *J. Natl. Cancer Inst.*, 90: 447–454, 1998.
- Hartenbach, E. M., Olson, T. A., Goswitz, J. J., Mohanraj, D., Twigg, L. B., Carson, L. F., and Ramakrishnan, S. Vascular endothelial growth factor (VEGF) expression and survival in human epithelial ovarian carcinomas. *Cancer Lett.*, 121: 169–175, 1997.
- Paley, P. J., Staskus, K. A., Gebhard, K., Mohanraj, D., Twigg, L. B., Carson, L. F., and Ramakrishnan, S. Vascular endothelial growth factor expression in early stage ovarian carcinoma. *Cancer* (Phila.), 80: 98–106, 1997.
- Olson, T. A., Mohanraj, D., Roy, S., and Ramakrishnan, S. Targeting the tumor vasculature: inhibition of tumor growth by a vascular endothelial growth factor-toxin conjugate. *Int. J. Cancer*, 73: 865–870, 1997.
- Nagy, J. A., Morgan, E. S., Herzberg, K. T., Manseau, E. J., Dvorak, A. M., and Dvorak, H. F. Pathogenesis of ascites tumor growth: angiogenesis, vascular remodeling, and stroma formation in the peritoneal lining. *Cancer Res.*, 55: 376–385, 1995.
- Simpson-Herren, L., Sanford, A. H., and Holmquist, J. P. Effects of surgery on the cell kinetics of residual tumor. *Cancer Treat. Rep.*, 60: 1749–1760, 1976.
- Luesley, D. M., Chan, K. K., Lawton, F. G., Blackledge, G. R., and Mould, J. M. Survival after negative second-look laparotomy. *Eur. J. Surg. Oncol.*, 15: 205–210, 1989.
- Luesley, D., Finn, C., and Varma, R. The role of surgery in epithelial ovarian cancer. *In: F. Sharp, W. P. Mason, and W. Creasman* (eds.), *Ovarian Cancer 2*, pp. 357–367. London, United Kingdom: Chapman & Hall, 1992.
- O'Reilly, M. S., Holmgren, L., Shing, Y., Chen, C., Rosenthal, R. A., Moses, M., Lane, W. S., Cao, Y., Sage, E. H., and Folkman, J. Angiostatin: a novel angiogenesis inhibitor that mediates the suppression of metastases by a Lewis lung carcinoma. *Cell*, 79: 315–328, 1994.

20. O'Reilly, M. S., Holmgren, L., Shing, Y., Chen, C., Rosenthal, R. A., Cao, Y., Moses, M., Lane, W. S., Sage, E. H., and Folkman, J. Angiostatin: a circulating endothelial cell inhibitor that suppresses angiogenesis and tumor growth. *Cold Spring Harbor Symp. Quant. Biol.*, *59*: 471–482, 1994.
21. Folkman, J. Angiogenesis inhibitors generated by tumors. *Mol. Med.*, *1*: 120–122, 1995.
22. Redlitz, A., Daum, G., and Sage, E. H. Angiostatin diminishes activation of the mitogen-activated protein kinases ERK-1 and ERK-2 in human dermal microvascular endothelial cells. *J. Vasc. Res.*, *36*: 28–34, 1999.
23. Sim, B. K., O'Reilly, M. S., Liang, H., Fortier, A. H., He, W., Madsen, J. W., Lapcevic, R., and Nacy, C. A. A recombinant human angiostatin protein inhibits experimental primary and metastatic cancer. *Cancer Res.*, *57*: 1329–1334, 1997.
24. Wu, Z., O'Reilly, M. S., Folkman, J., and Shing, Y. Suppression of tumor growth with recombinant murine angiostatin. *Biochem. Biophys. Res. Commun.*, *236*: 651–654, 1997.
25. Gorski, D. H., Mauceri, H. J., Salloum, R. M., Gately, S., Hellman, S., Beckett, M. A., Sukhatme, V. P., Soff, G. A., Kufe, D. W., and Weichselbaum, R. R. Potentiation of the antitumor effect of ionizing radiation by brief concomitant exposures to angiostatin. *Cancer Res.*, *58*: 5686–5689, 1998.
26. Lannutti, B. J., Gately, S. T., Quevedo, M. E., Soff, G. A., and Paller, A. S. Human angiostatin inhibits murine hemangioendothelioma tumor growth *in vivo*. *Cancer Res.*, *57*: 5277–5280, 1997.
27. Kirsch, M., Strasser, J., Allende, R., Bello, L., Zhang, J., and Black, P. M. Angiostatin suppresses malignant glioma growth *in vivo*. *Cancer Res.*, *58*: 4654–4659, 1998.
28. O'Reilly, M. S., Boehm, T., Shing, Y., Fukai, N., Vasios, G., Lane, W. S., Flynn, E., Birkhead, J. R., Olsen, B. R., and Folkman, J. Endostatin: an endogenous inhibitor of angiogenesis and tumor growth. *Cell*, *88*: 277–285, 1997.
29. Boehm, T., Folkman, J., Browder, T., and O'Reilly, M. S. Antiangiogenic therapy of experimental cancer does not induce acquired drug resistance. *Nature (Lond.)*, *390*: 404–407, 1997.
30. Dhanabal, M., Ramchandran, R., Volk, R., Stillman, I. E., Lombardo, M., Iruela-Arispe, M. L., Simons, M., and Sukhatme, V. P. Endostatin: yeast production, mutants, and antitumor effect in renal cell carcinoma. *Cancer Res.*, *59*: 189–197, 1999.
31. Volpert, O. V., Fong, T., Koch, A. E., Peterson, J. D., Waltenbaugh, C., Tepper, R. I., and Bouck, N. P. Inhibition of angiogenesis by interleukin 4. *J. Exp. Med.*, *188*: 1039–1046, 1998.
32. Dawson, D. W., Volpert, O. V., Gillis, P., Crawford, S. E., Xu, H., Benedict, W., and Bouck, N. P. Pigment epithelium-derived factor: a potent inhibitor of angiogenesis. *Science (Washington DC)*, *285*: 245–248, 1999.
33. O'Reilly, M. S., Pirie-Shepherd, S., Lane, W. S., and Folkman, J. Antiangiogenic activity of the cleaved conformation of the serpin antithrombin. *Science (Washington DC)*, *285*: 1926–1928, 1999.
34. Ramakrishnan, S., Olson, T. A., Bautch, V. L., and Mohanraj, D. Vascular endothelial growth factor-toxin conjugate specifically inhibits KDR/flk-1-positive endothelial cell proliferation *in vitro* and angiogenesis *in vivo*. *Cancer Res.*, *56*: 1324–1330, 1996.
35. Mohanraj, D., Olson, T., and Ramakrishnan, S. Expression of biologically active human vascular endothelial growth factor in yeast. *Growth Factors*, *12*: 17–27, 1995.
36. Carmichael, J., DeGraff, W. G., Gazdar, A. F., Minna, J. D., and Mitchell, J. B. Evaluation of a tetrazolium-based semiautomated colorimetric assay: assessment of chemosensitivity testing. *Cancer Res.*, *47*: 936–942, 1987.
37. Yoon, S. S., Eto, H., Lin, C. M., Nakamura, H., Pawlik, T. M., Song, S. U., and Tanabe, K. K. Mouse endostatin inhibits the formation of lung and liver metastases. *Cancer Res.*, *59*: 6251–6256, 1999.
38. Olson, T. A., Mohanraj, D., and Ramakrishnan, S. *In vivo* neutralization of vascular endothelial growth factor (VEGF)/vascular permeability factor (VPF) inhibits ovarian carcinoma-associated ascites formation and tumor growth. *Int. J. Oncol.*, *8*: 505–511, 1996.
39. Boehm, T., O'Reilly, M. S., Keough, K., Shiloach, J., Shapiro, R., and Folkman, J. Zinc-binding of endostatin is essential for its antiangiogenic activity. *Biochem. Biophys. Res. Commun.*, *252*: 190–194, 1998.
40. Boehm, T., Pirie-Shepherd, S., Trinh, L. B., Shiloach, J., and Folkman, J. Disruption of the KEX1 gene in *Pichia pastoris* allows expression of full-length murine and human endostatin. *Yeast*, *15*: 563–572, 1999.
41. Yamaguchi, N., Anand-Apte, B., Lee, M., Sasaki, T., Fukai, N., Shapiro, R., Que, I., Lowik, C., Timpl, R., and Olsen, B. R. Endostatin inhibits VEGF-induced endothelial cell migration and tumor growth independently of zinc binding. *EMBO J.*, *18*: 4414–4423, 1999.
42. Ji, W. R., Barrientos, L. G., Llinas, M., Gray, H., Villarreal, X., DeFord, M. E., Castellino, F. J., Kramer, R. A., and Trail, P. A. Selective inhibition by kringle 5 of human plasminogen on endothelial cell migration, an important process in angiogenesis. *Biochem. Biophys. Res. Commun.*, *247*: 414–419, 1998.
43. Lee, T. H., Rhim, T., and Kim, S. S. Prothrombin kringle-2 domain has a growth inhibitory activity against basic fibroblast growth factor-stimulated capillary endothelial cells. *J. Biol. Chem.*, *273*: 28805–28812, 1998.
44. O'Reilly, M. S., Holmgren, L., Chen, C., and Folkman, J. Angiostatin induces and sustains dormancy of human primary tumors in mice. *Nat. Med.*, *2*: 689–692, 1996.
45. Chang, Z., Choon, A., and Friedl, A. Endostatin binds to blood vessels *in situ* independent of heparan sulfate and does not compete for fibroblast growth factor-2 binding. *Am. J. Pathol.*, *155*: 71–76, 1999.
46. Moser, T. L., Stack, M. S., Asplin, I., Enghild, J. J., Hojrup, P., Everitt, L., Hubchak, S., Schnaper, H. W., and Pizzo, S. V. Angiostatin binds ATP synthase on the surface of human endothelial cells. *Proc. Natl. Acad. Sci. USA*, *96*: 2811–2816, 1999.
47. Dhanabal, M., Ramchandran, R., Waterman, M. J., Lu, H., Knebelmann, B., Segal, M., and Sukhatme, V. P. Endostatin induces endothelial cell apoptosis. *J. Biol. Chem.*, *274*: 11721–11726, 1999.
48. Mauceri, H. J., Hanna, N. N., Beckett, M. A., Gorski, D. H., Staba, M. J., Stellato, K. A., Bigelow, K., Heimann, R., Gately, S., Dhanabal, M., Soff, G. A., Sukhatme, V. P., Kufe, D. W., and Weichselbaum, R. R. Combined effects of angiostatin and ionizing radiation in antitumor therapy. *Nature (Lond.)*, *394*: 287–291, 1998.
49. Gorski, D. H., Beckett, M. A., Jaskowiak, N. T., Calvin, D. P., Mauceri, H. J., Salloum, R. M., Seetharam, S., Koons, A., Hari, D. M., Kufe, D. W., and Weichselbaum, R. R. Blockage of the vascular endothelial growth factor stress response increases the antitumor effects of ionizing radiation. *Cancer Res.*, *59*: 3374–3378, 1999.